

# Phosphating treatment and corrosion properties of Mg–Mn–Zn alloy for biomedical application

Liping Xu · Erlin Zhang · Ke Yang

Received: 26 January 2008 / Accepted: 3 November 2008 / Published online: 26 November 2008  
© Springer Science+Business Media, LLC 2008

**Abstract** A phosphating treatment was applied to Mg–Mn–Zn alloy in order to improve the corrosion resistance. Surface morphology and phase constitute were observed and identified by SEM, EDS, SAXS, XRD and XPS. SEM observation showed that a rough and crystalline reaction layer was formed on the surface of Mg alloy. With the increasing of phosphating time, the layer became thicker and denser. It has been showed that the reaction layer was mainly composed of brushite ( $\text{CaHPO}_4 \cdot 2\text{H}_2\text{O}$ ). Small amount of  $\text{Zn}^{2+}$  was also detected by XPS and EDS. The corrosion resistance of the phosphated samples was measured by the electrochemical polarization and the immersion test in comparison with the bare alloy. The results manifested that the corrosion resistance of Mg alloy was improved by the phosphating treatment, and the corrosion resistance increased with the increase of the phosphating time within 50 min. Immersion tests showed that the phosphate layer could protect magnesium alloy from fast corrosion. The brushite layer has been transformed into hydroxyapatite (HA) during the immersion in the simulated body fluid (SBF) solution,

which suggested the brushite layer could provide good biocompatibility.

## 1 Introduction

Magnesium alloys have shown potential application for biodegradable materials due to their outstanding biological performance [1] and biodegradability in bioenvironment [2–4]. Mechanical properties of magnesium alloys are much close to those of human bone in the case for commonly used artificial implant materials. Thus, the stress shielding effects existed between other biometallic bone implants made of titanium alloys or stainless steels, and bone tissue could be reduced or avoided completely. In addition, due to their biodegradability, the second surgery for the removal of the metal bone plates and screws might be avoided in the case of magnesium implants. However, rapid corrosion of magnesium and its alloys in chloride containing solutions including the human body fluid or blood plasma limited their clinical applications [5, 6]. For instance, the alloys lost mechanical integrity before the sufficient heal of bone tissue and produced hydrogen gas in the corrosion process [3, 6]. Therefore, it is very important to improve the corrosion resistance of magnesium alloys for their biomedical application. On the other hand, no report so far has been published to show that magnesium alloys have good surface osteoconductivity and osteoinductivity although the new bone tissue was observed around magnesium implant after 5 weeks implantation [4].

Many coating techniques have been developed in industry to protect magnesium alloys from sea water corrosion attack, such as chromate coating, phosphate-permanganate coating, rare earth conversion coating and so on [7–11]. But these studies mainly focused on magnesium

---

L. Xu · E. Zhang (✉) · K. Yang  
Institute of Metal Research, Chinese Academy of Sciences,  
Shenyang 110016, China  
e-mail: erlin.zhang@imr.ac.cn

L. Xu  
Graduate University of Chinese Academy of Sciences,  
Beijing 100049, China

E. Zhang  
School of Materials Science and Engineering,  
Jiamusi University, Jiamusi 154007, China

alloys as structural materials in automotive and aeronautical applications instead of biomedical engineering applications. Other researches on biomedical magnesium alloys have shown that aluminium coating improved the corrosion resistance of magnesium alloy [12, 13], but aluminium coating was not suitable for biomedical application since aluminium was reported to have potential metal toxicity to human body. Titanium coating was also deposited by ion plating on magnesium surface in order to improve both corrosion properties and biocompatibility [14]. The corrosion rate was reduced by this titanium coating as proposed, but the titanium coating was not biodegradable.

For the industrial application, phosphating treatment on magnesium can provide corrosion protection against sea water attack, and are normally used as a pretreatments prior to a final sealing process. Kouisni et al. [10] studied the formation and the growth of protective zinc phosphate film contained  $Zn_3(PO_4)_2 \cdot 4H_2O$  on an AM60 magnesium alloy in a phosphating bath mainly containing  $Na_2HPO_4$ ,  $H_3PO_4$  and  $Zn(NO_3)_2$ . Li et al. [11] obtained a zinc phosphate coating on AZ91D magnesium alloy in a phosphating bath with  $H_3PO_4$ , ZnO and NaF as main ingredients. Han et al. [15] also obtained a phosphate film of  $Mn_3(PO_4)_2$  on AZ31D alloy in a bath containing phosphate and manganese. All these phosphate coatings have shown good protection for magnesium alloys against fast corrosion in NaCl solution, but no result so far showed that  $Zn_3(PO_4)_2 \cdot 4H_2O$  or  $Mn_3(PO_4)_2$  has good biocompatibility.

Previous in vivo study on magnesium alloy implant has shown that a phosphate layer formed in vivo on the surface after 4–5 weeks postimplantation [4]. It was believed that this phosphate layer protected magnesium implant from fast corrosion or degradation, and on the other hand induced the formation of the new bone on the surface of the magnesium alloy implant [4]. Other study on biomedical titanium biomedical material has shown the brushite ( $CaHPO_4 \cdot 2H_2O$ ) coatings on the surface of titanium have the propensity for promoting bone growth [16]. In addition, low concentration of  $Zn^{2+}$  was believed to stimulate osteoblastic cell proliferation and bone formation [17, 18]. Therefore, it is reasonably believed that brushite coating with small amount of Zn can improve the surface bone tissue biocompatibility of magnesium alloy.

In this paper,  $Ca(H_2PO_4)_2 \cdot H_2O$  and  $Zn(H_2PO_4)_2 \cdot 2H_2O$  were chosen as main components of a new phosphating bath in order to form a brushite coating with small amount of Zn on the surface of Mg–Mn–Zn alloy. It is purposed that the brushite coating can improve the corrosion resistance, but also can improve surface biocompatibility of magnesium alloy. Primary results focused on the characterization and the corrosion protection of the brushite coating.

## 2 Experimental

### 2.1 Sample preparation

Extruded Mg–Mn–Zn (Mg–1.2Mn–1.0Zn, in wt%) bars were prepared in our laboratory. For electrochemical polarization test, specimens were cut from the extruded bar and moulded into epoxy resin with only one side of  $1\text{ cm}^2$  exposed. The sample surfaces were ground with SiC emery papers of up to 2,000 grits, then ultrasonically cleaned in alcohol for 5 min and dried in warm air. For immersion test, plate samples with a dimension of 10 mm in diameter and 3 mm in thickness were cut from the extruded bar, and moulded into epoxy resin with only one side exposed and ground with SiC emery paper of up to 2,000 grits, then ultrasonically cleaned in alcohol for 5 min and dried in warm air.

### 2.2 Phosphating treatment

The samples were first immersed in an alkaline solution at  $63^\circ\text{C}$  for 15 min for degreasing and subsequently immersed in a mixed acid solution (2%) of  $H_3PO_4$  and  $H_2SO_4$  at room temperature for 5 s for surface activation. Then, the samples were treated in a phosphating bath for 10 min, 20 min, 30 min and 50 min, respectively. The ingredients of the phosphating bath were listed in Table 1. The pH of the bath was adjusted by  $H_3PO_4$  or NaOH to around 4.00–4.50. The phosphating temperature was  $60\text{--}65^\circ\text{C}$ .

### 2.3 Electrochemical polarization test

Both the phosphated and the non-phosphated samples (bare samples) were used in electrochemical test. Electrochemical tests were carried out at  $37^\circ\text{C} \pm 1^\circ\text{C}$  in 0.9% NaCl solution using a CHI660A Electrochemical workstation (CH Instruments Inc. USA). The tests were carried out in a beaker containing 350 ml solution using a standard three-electrode configuration: the saturated calomel as a reference, a platinum electrode as the counter and the sample as the working electrode. In the potentiodynamic polarization tests, the working electrode was first immersed in the solution for 10 min and then the polarization curve was measured at a scanning rate of 0.3 mV/s.

**Table 1** Chemical compositions of the phosphating bath

Composition	Concentration
Phosphoric acid	6–8 ml/l
$Ca(H_2PO_4)_2 \cdot H_2O$	7.92 g/l
$Zn(H_2PO_4)_2 \cdot 2H_2O$	1.55 g/l
$NaNO_3$	1–3 g/l
$NaNO_2$	2–5 g/l

### 2.4 Immersion in SBF solution

Both the phosphated and the bare samples were immersed in 12 ml SBF (the ratio of the surface area to solution volume is 1 cm<sup>2</sup>:15 ml) at 37°C ± 1°C for 1, 2, 4 and 9 days, respectively. The ion concentration of SBF solution was list in Table 2. Then the samples were washed in distilled water. The pH value of the solution was measured before and after the immersion by a pH meter with an accuracy of 0.01 to calculate the change of the pH value. Before immersion, the pH of the SBF solution was adjusted to 7.40 by HCl and (CH<sub>2</sub>OH)<sub>3</sub>CNH<sub>2</sub>.

### 2.5 Microstructure

The microstructure of the phosphated samples was observed on a SSX-550 scanning electronic microscopy (SEM). The chemical composition of the phosphated layer was determined by energy dispersive spectrum (EDS). Surface structure of the phosphated samples was characterized by X-ray photoelectron spectroscopy (XPS, Escalab250, Thermo Corp.). The XPS measurements were performed using an X-ray source of Al K $\alpha$  (1486.68 eV). Measured binding energies were corrected by referring the binding energy of C<sub>1s</sub> of methylene groups of the hydrocarbon (284.6 eV) absorbed on the surface of the samples. In order to identify the phase constitutes of the phosphated product on the magnesium samples, the surface was examined with small angle X-ray scanning (SAXS) which was conducted on a X-ray diffractometer (XRD, D/MAX-RB, Rigaku) with an incident angle of 2 degree against the surface of the specimens, and the measurements were performed with a continuous scanning mode at a rate of 4°/min. In order to identify the phase transformation of the phosphated layer, X-ray diffraction on the surface of the phosphated sample after immersion in SBF solution for 9 days was conducted on an X-ray diffractometer (XRD, Dmax-2500PC, Rigaku). After being washed in distilled water, the surface morphologies of samples after immersion were also observed by SEM and the chemical compositions of the samples after immersion for 9 days were determined by EDS.

## 3 Results

### 3.1 Phase identification and microstructure

Appearance observation shows that the magnesium sample was covered partially by a gray film after 10 min

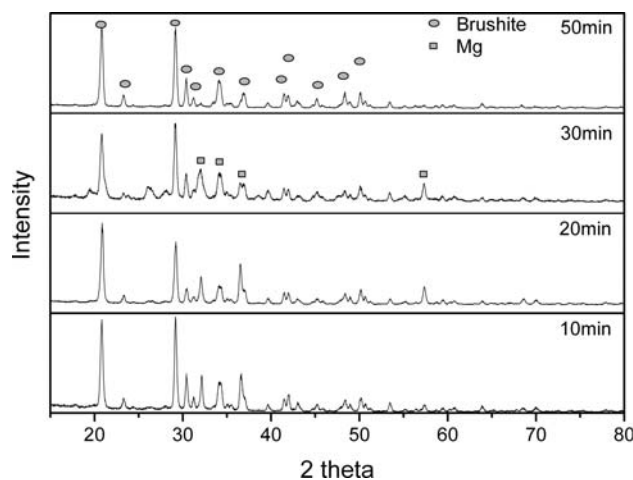
**Table 2** Ion concentrations of SBF

Ion	Na <sup>+</sup>	K <sup>+</sup>	Mg <sup>2+</sup>	Ca <sup>2+</sup>	Cl <sup>-</sup>	HCO <sub>3</sub> <sup>-</sup>	HPO <sub>4</sub> <sup>2-</sup>	SO <sub>4</sub> <sup>2-</sup>
Concentration (mM/l)	142.0	5.0	1.5	2.5	147.8	4.2	1.0	0.5

phosphating treatment and completely after more than 20 min treatment. In order to identify the phase constitute of the reaction film, a small angle X-ray scanning (SAXS) was conducted on the magnesium surfaces which had been treated for different time, as shown in Fig. 1. After 10 min phosphating, a large amount of brushite (CaHPO<sub>4</sub> · 2H<sub>2</sub>O) phases were detected in the surface layer. The diffraction peaks of magnesium matrix also presented in the pattern. With the increasing of the phosphating time, no other new phase except brushite can be identified by X-ray diffraction. In addition, the intensity of Mg diffraction peaks decreases with the increasing of the phosphating time, indicating that the phosphating layer became thicker and thicker with the phosphating time.

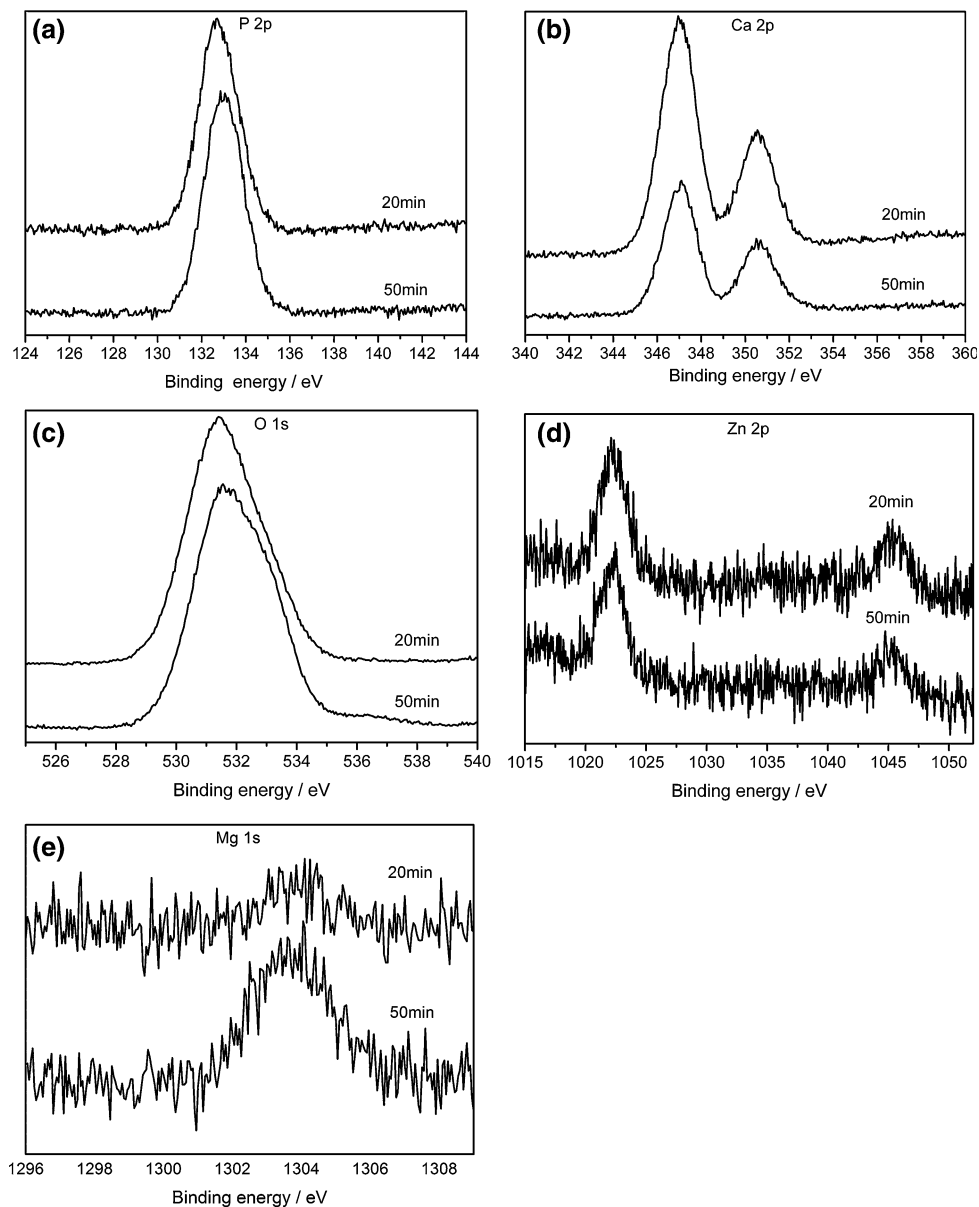
Figure 2 shows the P<sub>2p</sub>, Ca<sub>2p</sub>, O<sub>1s</sub>, Zn<sub>2p</sub> and Mg<sub>1s</sub> XPS spectrum of the magnesium surface phosphated in bath for 20 min and 50 min. It can be seen that P<sub>2p3/2</sub> spectrum was detected as single peak and Ca<sub>2p</sub> spectra were detected as doublet peaks. From the binding energies of P<sub>2p3/2</sub> and Ca<sub>2p</sub>, it can be concluded that P element existed in the layer in a form of phosphate. O<sub>1s</sub> was detected as single peak. Zn<sub>2p</sub> spectra were detected as doublet peaks. Small amount of Mg was also detected by XPS. In addition, with the increasing of the phosphating time from 20 min to 50 min, no shift of any spectra peaks was observed. Combined with the SAXS results shown in Fig. 1, it can be concluded that the surface layer is mainly composed of brushite.

Figure 3 shows the surface morphology of the phosphate film formed on the magnesium alloy phosphated for 10 min. It can be seen that lots of regular crystal phases



**Fig. 1** SAXS diffraction patterns on the surfaces of Mg alloys after phosphating treatment for 10 min, 20 min, 30 min and 50 min, respectively

**Fig. 2** XPS spectra of the magnesium alloy samples phosphated for 20 min and 50 min. **a** P<sub>2p</sub>, **b** Ca<sub>2p</sub>, **c** O<sub>1s</sub>, **d** Zn<sub>2p</sub> and **e** Mg<sub>1s</sub>



with small particles phases on the surface were found on the magnesium surface after 10 min phosphating. EDS analysis was conducted on the crystal phase and the small particle, as shown in Fig. 4. EDS analysis indicates that the crystal is mainly composed of O, P and Ca, and the particle consists mainly of O, Na, P, Ca and Zn. Combined with the SAXS results in Fig. 1 and XPS results in Fig. 2, it can be concluded that the crystal phases are brushite and the particle phases are mixture of several compounds precipitated from the solution. However, the amount of these compounds is too small to be detected and identified by XRD. With the increasing of the phosphating time, no difference in the surface morphology of the phosphate films can be found (not shown here).

### 3.2 Electrochemical polarization test

In order to assess the protection of the phosphating film on magnesium alloy against corrosion, electrochemical polarization tests were conducted on the magnesium alloy samples with and without phosphating treatment. The polarization curves of the magnesium alloys with and without phosphating treatment are shown in Fig. 5. The electrochemical parameters obtained from Fig. 5 are listed in Table 3. The most negative corrosion potential ( $E_{\text{corr}}$ ) was obtained for the bare sample, which also exhibited the highest corrosion current density ( $i_{\text{corr}}$ ). All of the phosphated samples exhibit a more positive  $E_{\text{corr}}$ , a higher corrosion resistance ( $R_p$ ) and a lower  $i_{\text{corr}}$  than the bare

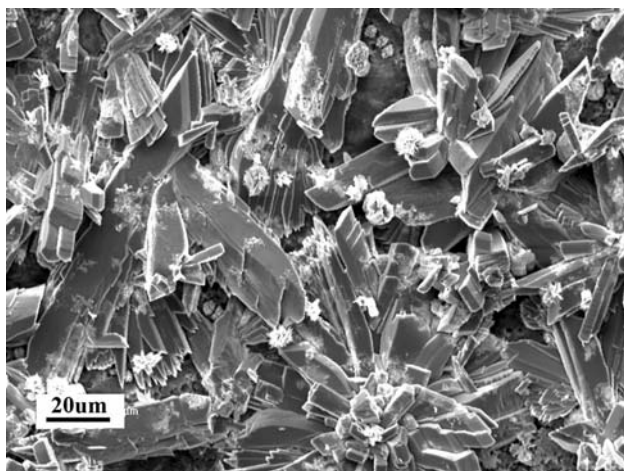


**Fig. 3** SEM surface morphology of the magnesium alloy sample after phosphating treatment for 10 min

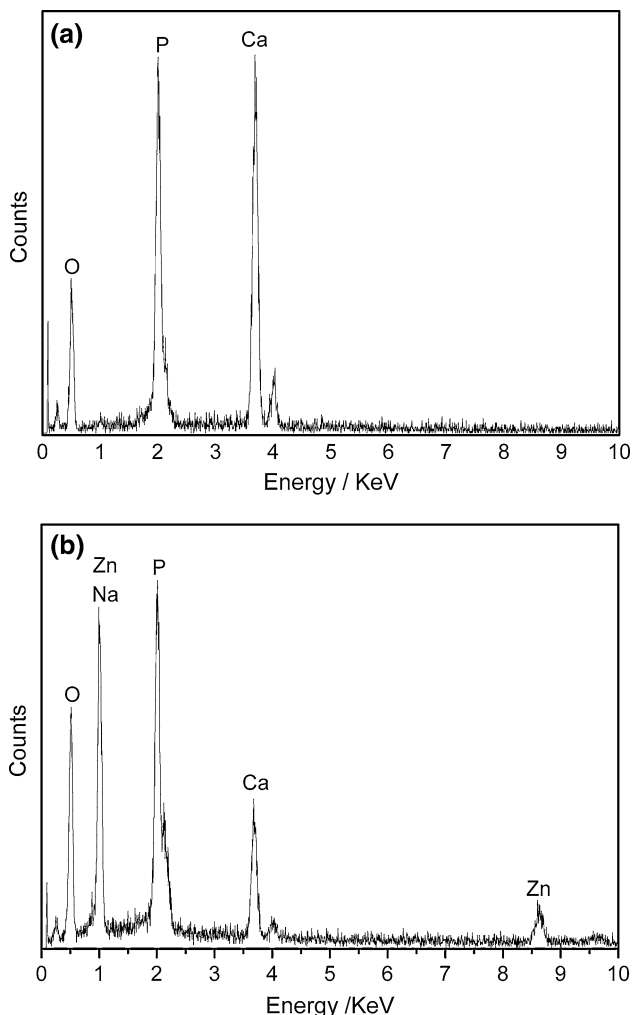


**Fig. 4** EDS analysis on **a** the crystal phase and **b** the small particles on the magnesium alloy phosphated for 10 min

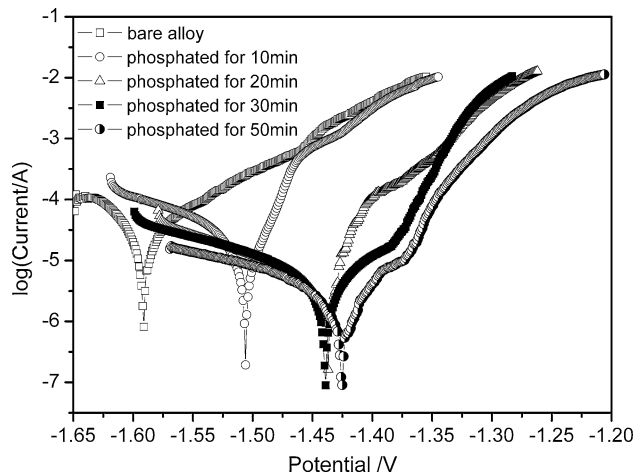


**Fig. 5** The electrochemical polarization curves of the bare magnesium alloy and the phosphated samples in 0.9 wt% NaCl solution

sample, indicating that the phosphating treatment moves the  $E_{corr}$  to a more noble position and increases the corrosion resistance. E.g. after phosphating for 20 min, the  $E_{corr}$  value was changed from  $-1.591$  V to  $-1.437$  V, and the corrosion resistance was increased from  $469.5 \Omega$  to  $2,178 \Omega$ . It can also be found that the longer the phosphating time is, the lower the  $i_{corr}$  is and the higher the  $R_p$  is, as listed in Table 3. However, further extension of treatment time after 20 min did not change  $E_{corr}$  and  $R_p$  significantly as it did in the first 20 min.

### 3.3 Immersion in SBF solution

The pH values of the SBF solutions in which the bare and the phosphated magnesium (for 30 min) alloy samples were immersed are shown in Fig. 6 against the immersion time. For both the bare samples and the phosphated samples, pH values increase with the immersion time. However, the increase of the pH value of the SBF solution containing the phosphated samples is slower than that of the solutions containing the bare samples. After 1 day immersion, the pH value of the solutions containing the bare samples was about 8.17 while the pH value of the

**Table 3** The parameters of the electrochemical polarization tests in 0.9 wt% NaCl solution

Samples	$i_{corr}$ $\mu A/cm^2$	$E_{corr}$ V	$R_p$ $\Omega$
Bare alloy	41.05	-1.591	469.5
Phosphated for 10 min	13.41	-1.506	847.8
Phosphated for 20 min	7.18	-1.437	2,178
Phosphated for 30 min	4.63	-1.439	3,801
Phosphated for 50 min	2.96	-1.425	4,976

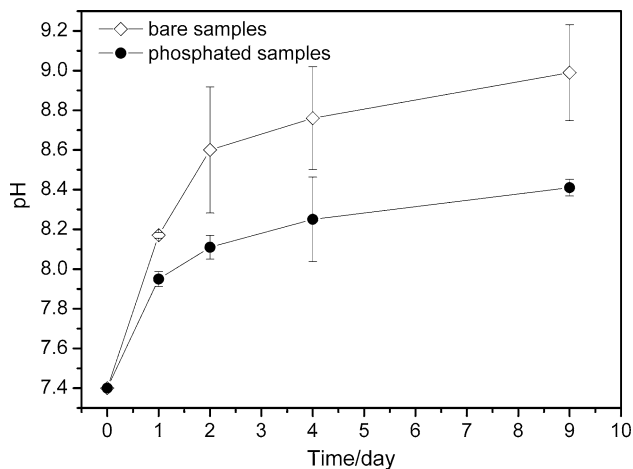


**Fig. 6** Change in the pH value of SBF solutions containing the bare samples and the phosphated samples (30 min) with the immersion time

solution containing the phosphated samples was about 7.95. After 2, 4 and 9 days immersion, the difference in pH between the solutions containing the phosphated samples and the bare samples is as high as 0.5 unit.

Figure 7 shows the surface morphologies of the bare samples after immersion in SBF for different durations. After 1 day immersion, the surface of the bare sample was covered by a corrosion layer with many cracks on the surface. Some white particles were also deposited on the corroded surface. With the increasing of the immersion time, more and more particles were observed. EDS analysis was conducted on the corrosion layer and the particles after 9 days immersion, and the element quantitative analysis results are listed in Table 4. The results indicate that both the corrosion product and the deposition particles are mainly composed of O, P, Mg, Ca and small amount of Na. The ratios of Ca to P (Ca/P) are less than 0.8, which is much lower than that of hydroxyapatite (HA).

The surface morphologies of the phosphated samples after immersion in SBF solution for different durations are

**Table 4** EDS analysis results on the surface of the bare alloy immersed for 9 days (at%)

Elements	O	Na	Mg	P	Ca	Ca/P
Corrosion layer	77.385	0.561	3.519	13.372	5.163	0.386
Particle	75.146	0.575	7.730	9.207	7.342	0.797

shown in Fig. 8. After 1 day immersion, partial brushite crystals lost their shape edges and corners, as marked by the arrow in Fig. 8a), indicating that the brushite crystals on the surface of magnesium sample began to dissolve in SBF. Also some white particles were found on the surface. After 2 days immersion, no obvious difference in the surface morphology was observed by SEM compared to that immersed for 1 day. After 4 days immersion, more and more brushite crystals were dissolved, as shown in Fig. 8b). Nine days later, there were cracks on the surface of the sample, displaying the brushite dissolved and became many smaller parts. Meanwhile, more particles were found on the surface. EDS analysis was conducted on the dissolving brushite and the deposited particle after 9 days immersion, and the element quantitative analysis results are listed in Table 5. The results disclose that the dissolving brushite layer is mainly composed of P, O, Ca and tiny amount of Mg, and the Ca/P ratio is 1.467, close to that of calcium phosphates. The particles deposited on the surface are mainly composed of O, P, Mg, Ca and Na, and the Ca/P ratio is 1.292. In order to identify the phase transformation of the brushite layer during the immersion, XRD was conducted on the surface of the phosphated sample after immersion in SBF solution for 9 days, as shown in Fig. 9. The XRD pattern of Mg–Mn–Zn alloy before the phosphating treatment and the standard JCPDS patterns of brushite and HA were also shown for comparison. It can be found that HA phase as well as magnesium matrix were detected, but the brushite phase completely disappeared, displaying that the brushite was transformed to HA during the immersion.

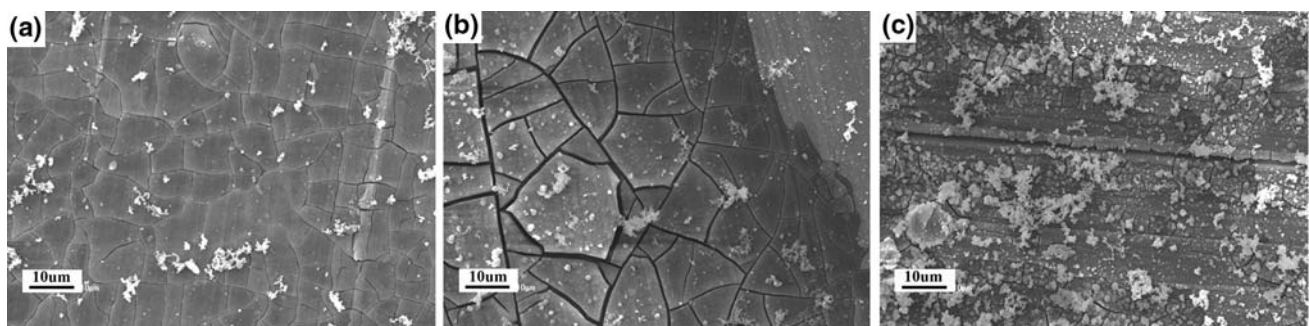


**Fig. 7** Surface morphology of the bare samples immersed in SBF solution for **a** 1 day, **b** 2 days and **c** 9 days

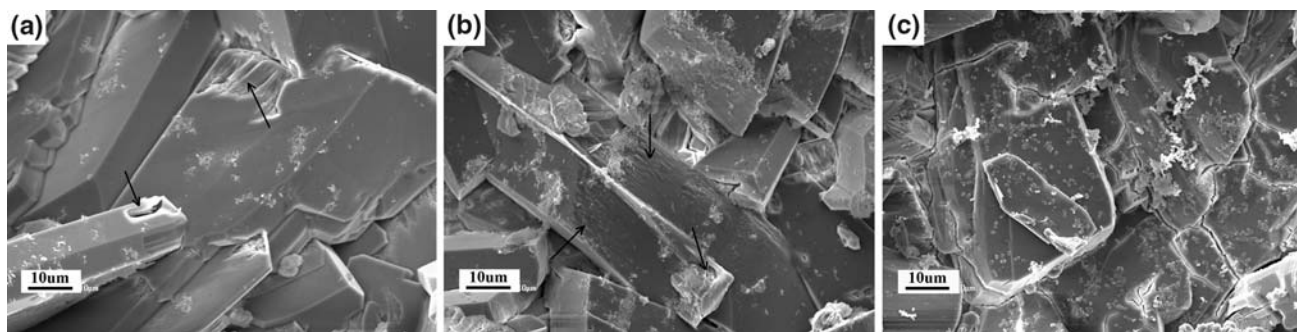


**Fig. 8** Surface morphology of the phosphated samples (30 min) immersed in SBF solution for **a** 1 day, **b** 4 days and **c** 9 days

**Table 5** EDS analysis results on the surface of the phosphated sample immersion for 9 days (at%)

Elements	O	Na	Mg	P	Ca	Ca/P
Dissolving brushite	70.030	–	0.753	11.841	17.376	1.467
Deposited particle	77.022	4.992	1.572	7.199	9.305	1.292

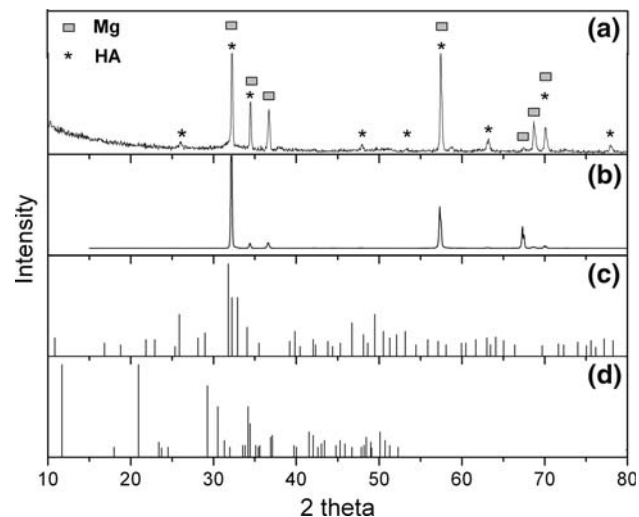


**Fig. 9** XRD diffraction pattern on the surface of the phosphated Mg alloy sample after immersion in SBF for 9 days. (a) the phosphated Mg alloy sample, (b) Mg–Mn–Zn substrate, (c) HA(JCPDS09-0432), (d) brushite (JCPDS09-0077)

**4 Discussion**

**4.1 Phosphating reaction**

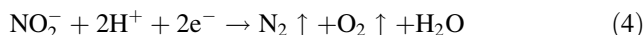
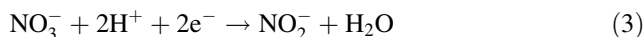
Mg is a relatively active alloy, which easily reacts with lots of solutions, especially Cl<sup>-</sup> ion containing solutions. Microstructure on the magnesium alloy which was immersed in the phosphating bath clearly shows that most of the surface was covered by a slab-like phosphate crystal after phosphatization of 10 min as shown in Fig. 3. After 20 min, the magnesium alloy surface was fully covered by the phosphate. These results indicate that a reaction

happened on the surface of the Mg alloy samples. EDS, SAXS and XPS results indicate that the coating is mainly composed of O, P, Ca, and a little Mg, Zn and Na and the main phase constitute is brushite.

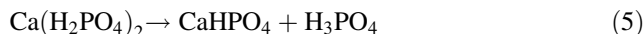
When Mg alloy is immersed into the phosphating bath, magnesium alloy will dissolve in the solution through the following reactions:



As a result, hydrogen will be released from the solution. On the other hand, in the phosphating bath, NO<sub>3</sub><sup>-</sup> and NO<sub>2</sub><sup>-</sup> can react with H<sup>+</sup> through following reactions,



Reactions (3) and (4) consume H<sup>+</sup> quickly, so the local pH at the metal-solution interface increases and facilitates the precipitation of insoluble phosphate [10]. Thus, following reactions happen at the surface of the magnesium alloy,



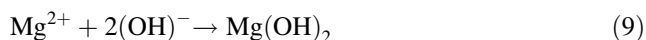
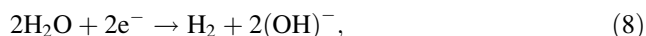
As a result, brushite will be formed on the surface of the magnesium alloy. As discussed above, besides brushite phases, some particles which consist of several phosphate compounds were also formed on the surface of the Mg alloy. In other studies on the phosphating technology, Zn<sub>2</sub>Ca(PO<sub>4</sub>)<sub>2</sub> · 2H<sub>2</sub>O [19] and MgZn<sub>2</sub>(PO<sub>4</sub>)<sub>2</sub> [11] were detected in the phosphated layer. It is believed that these phosphate compounds were precipitated from solution during the phosphating process or when the samples were taken out. Unfortunately the molecular formula can not be identified by XRD in this study.

**4.2 Corrosion resistance**

The noble E<sub>corr</sub> and the high Rp obtained from the electrochemical measurement of the phosphated samples

demonstrate that a passive layer was formed on the magnesium alloy surface which provided effective protection to the substrate. The pH value of SBF containing the bare samples increased fast from 7.40 to 8.60 in the first 2 days, while the pH value of the solution containing the phosphated samples was 8.41 after 9 days immersion. From the pH change of the immersion test, it can be concluded the phosphating layer is beneficial to the mitigation of the corrosion process of the Mg alloy substrate in the SBF during 9 days immersion time.

For the bare sample, when the sample is exposed to SBF, general corrosion in aqueous solutions takes place as followings [20]:

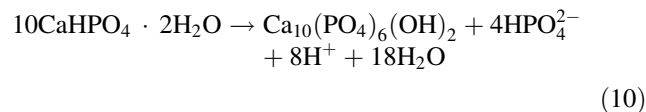


Chloride ions can transform the  $\text{Mg}(\text{OH})_2$  into more soluble  $\text{MgCl}_2$  [20–22]. Thus, large amount of Mg ions dissolve in the test solution and lead to the increase in the pH value. In general, apatite or other calcium phosphates will form on the surface of some biomaterials such as chemically treated Ti alloy and bioglass in SBF because SBF is a solution slightly supersaturated by calcium and phosphate ions. However, it was believed that magnesium has considerable inhibitory effect on the formation and growth of HA and other crystalline calcium phosphates [23], and on the direct precipitation of HA from low supersaturation solution [24] because of the adsorption of magnesium on active growth sites [25, 26] and the incorporation of  $\text{Mg}^{2+}$  into the precipitate [27]. Therefore, in the SBF containing the bare samples, the high Mg ion concentration due to the corrosion of magnesium alloy depresses the precipitation of apatite or other calcium phosphate, but accelerates the precipitation of Mg, Ca containing phosphates on the surface of magnesium alloy. However, the slow increase in the pH value of the SBF solution after 2 days immersion, as shown in Fig. 6 indicates the Mg and Ca containing phosphate corrosion layer can also prevent the corrosion to some extent.

For the phosphated samples, the brushite layer provides an effective protection for the magnesium alloy as discussed above. However, the crystalline phosphate coatings are generally porous, and the solution can still contact with substrates through the pores among the brushite crystals. Thus the phosphated samples were not protected completely. Therefore, the phosphate coating does not stop the degradation of magnesium alloy in SBF solution completely, but reduce the degradation of magnesium alloy.

After the immersion in SBF solution for 9 days, EDS analysis results showed the brushite layer tended to be transformed into a high Ca/P ratio phase and the XRD results indicated that the high Ca/P ratio phase was HA although

there was little difference in the surface microstructure before and after the immersion, as shown in Figs. 3 and 8. The phase transformation might take place as follows:



The dissolution of the brushite and the transformation of brushite into HA will release acidic phosphate ions into surrounding environment, which will resist the increase in the pH. This characteristic will decrease the local alkalization around magnesium implant in vivo. From this point of view, brushite coating is very suitable to be a protective and biocompatible coating for the biodegradable magnesium alloy.

#### 4.3 Surface biocompatibility

Above results and discussion clearly show that brushite coatings have successfully formed on the surface of Mg–Mn–Zn alloys and provide effective protection to Mg alloys against the corrosion of SBF solution. Brushite has exhibited excellent biocompatibility as bone substitute materials, and has been successfully applied to the bioactive layer of Ti and its alloys [28, 29] and to the bone cement [30–33]. The immersion test clearly shows that the brushite has the tendency to be transformed into HA phase after immersion in SBF for 9 days, as proven by other studies that brushite might be a precursor phase in the native mineralization process in the formation of bone apatite in vivo [34–37]. The presence of small amount of  $\text{Zn}^{2+}$  in the coating will also improve the biocompatibility of the coating because zinc is an essential trace element that plays important roles in controlling the function of osteoblast significantly and increasing osteoblasts adhesion and alkaline phosphatase activity of bone cells [18]. In addition, the release of acidic phosphate ions during the transformation into bone apatite will neutralize alkalization effect caused by corroding magnesium which is not desirable at all in the application of Mg alloys as biomedical materials.

All of these suggest that magnesium alloys with brushite coating would show better biocompatibility than bare alloys. The brushite coatings on Mg alloy might not only improve the corrosion resistance but also promote the bone growth for biodegradable implant application. Further studies are continuing for the purpose of assessing the biocompatibility of brushite coating on the magnesium.

## 5 Conclusion

A brushite coating on the Mg–Mn–Zn alloy was successfully obtained by a phosphating process for biomedical



purpose. Both electrochemical tests and immersion tests showed that the brushite coating provided good protection to the Mg alloy substrate against SBF corrosion. However, the brushite coating did not completely stop the corrosion or degradation of magnesium in SBF, but reduced the corrosion rate or degradation rate. As a surface coating layer, the brushite coating can improve the surface biocompatibility of Mg alloy substrate due to the fact that the brushite coating tended to be transformed into HA phase and the release of acidic phosphate ions neutralized alkalization effect caused by the corrosion of magnesium to some extent.

**Acknowledgements** One of authors (ErLin Zhang) would like to acknowledge the financial support from the Institute of Metal Research (IMR), Chinese Academy of Sciences (CAS), Shenyang Science and Technology Institute (Program No. 1062109-1-00), and Heilongjiang Provincial Natural Science Fund (E2007-18).

## References

- G. Song, Corros. Sci. **49**, 1696 (2007). doi:10.1016/j.corsci.2007.01.001
- F. Witte, J. Fischer, J. Nellesen, H.-A. Crostack, V. Kaese, A. Pisch, F. Beckmann, H. Windhagen, Biomaterials **27**, 1013 (2006). doi:10.1016/j.biomaterials.2005.07.037
- F. Witte, V. Kaese, H. Haferkamp, E. Switzer, A. Meyer-Lindenberg, C.J. Wirth, H. Windhagen, Biomaterials **26**, 3557 (2005). doi:10.1016/j.biomaterials.2004.09.049
- L. Xu, G. Yu, E. Zhang, F. Pan, K. Yang, J. Biomed. Mater. Res. A **83A**, 703 (2007). doi:10.1002/jbm.a.31273
- G. Song, Adv. Eng. Mater. **7**, 563 (2005). doi:10.1002/adem.200500013
- M.P. Staiger, A.M. Pietak, J. Huadmai, G. Dias, Biomaterials **27**, 1728 (2006). doi:10.1016/j.biomaterials.2005.10.003
- J.E. Gray, B. Luan, J. Alloy. Comp. **336**, 88 (2002). doi:10.1016/S0925-8388(01)01899-0
- A.L. Rudd, C.B. Breslin, F. Mansfeld, Corros. Sci. **42**, 275 (2000). doi:10.1016/S0010-938X(99)00076-1
- M. Zhao, S. Wu, J. Luo, Y. Fukuda, H. Nakae, Surf. Coat. Tech. **200**, 5407 (2006). doi:10.1016/j.surfcoat.2005.07.064
- L. Kouisni, M. Azzi, M. Zertoubi, F. Dalard, S. Maximovitch, Surf. Coat. Tech. **185**, 58 (2004). doi:10.1016/j.surfcoat.2003.10.061
- L.Y. Niu, Z.H. Jiang, G.Y. Li, C.D. Gu, J.S. Lian, Surf. Coat. Tech. **200**, 3021 (2006). doi:10.1016/j.surfcoat.2004.10.119
- L.H. Chiu, H.A. Lin, C.C. Chen, C.F. Yang, C.H. Chang, J.C. Wu, Mater. Sci. Forum **419–422**, 909 (2003)
- L.-H. Chiu, C.-C. Chen, C.-F. Yang, Surf. Coat. Tech. **191**, 181 (2005). doi:10.1016/j.surfcoat.2004.02.035
- E. Zhang, L. Xu, K. Yang, Scr. Mater. **53**, 523 (2005). doi:10.1016/j.scriptamat.2005.05.009
- E.H. Han, W.Q. Zhou, D.Y. Shan, W. Ke, Mater. Sci. Forum **419–422**, 879 (2003)
- J. Redepinning, T. Schlessinger, S. Burnham, L. Lippiello, J. Miyano, J. Biomed. Mater. Res. A **30**, 287 (1996). doi:10.1002/(SICI)1097-4636(199603)30:3<287::AID-JBM3>3.0.CO;2-M
- A. Grandjean-Laquerriere, P. Laquerriere, E. Jallot, J.-M. Nedelec, M. Guenounou, D. Laurent-Maquin, T.M. Phillips, Biomaterials **27**, 3195 (2006). doi:10.1016/j.biomaterials.2006.01.024
- M. Yamaguchi, H. Oishi, Y. Suketa, Biochem. Pharmacol. **36**, 4007 (1987). doi:10.1016/0006-2952(87)90471-0
- G. Lorin, *Phosphating of metals* (Finishing Publications LTD, Hampton Hill, 1974)
- G.L. Makar, J. Kruger, Int. Mater. Rev. (USA) **38**, 138 (1993)
- H. Altun, S. Sen, Mater. Des. **25**, 637 (2004)
- K.R. Baldwin, D.J. Bray, G.D. Howard, R.W. Gardiner, Mater. Sci. Tech.-Lond. **12**, 937 (1996)
- N.C. Blumenthal, Clin. Orthop. Relat. Res. **247**, 279 (1989)
- K.S. TenHuisen, P.W. Brown, J. Biomed. Mater. Res. **36**, 306 (1997). doi:10.1002/(SICI)1097-4636(19970905)36:3<306::AID-JBM5>3.0.CO;2-I
- Z. Amjad, P.G. Koutsoukos, G.H. Nancollas, J. Colloid. Interface Sci. **101**, 250 (1984). doi:10.1016/0021-9797(84)90025-0
- G.H. Nancollas, B. Tomazic, M. Tomson, Croat. Chem. Acta **48**, 431 (1976)
- E.D. Eanes, S.L. Rattner, J. Dent. Res. **60**, 1719 (1981)
- R.Z. LeGeros, Clin Orthop. Relat. Res. **395**, 81 (2002). doi:10.1097/00003086-200202000-00009
- J. Redepinning, J.P. McIsaac, Chem. Mater. **2**, 625 (1990). doi:10.1021/cm00012a001
- F. Theiss, D. Apelt, B. Brand, A. Kutter, K. Zlinszky, M. Bohner, S. Matter, C. Frei, J.A. Auer, B. von Rechenberg, Biomaterials **26**, 4383 (2005). doi:10.1016/j.biomaterials.2004.11.056
- Z. Xia, L.M. Grover, Y. Huang, I.E. Adamopoulos, U. Gbureck, J.T. Triffitt, R.M. Shelton, J.E. Barralet, Biomaterials **27**, 4557 (2006). doi:10.1016/j.biomaterials.2006.04.030
- B. Flautre, C. Maynou, J. Lemaitre, P.V. Landuyt, P. Hardouin, J. Biomed. Mater. Res. B Appl. Biomater. **63**, 413 (2002). doi:10.1002/jbm.10262
- D. Apelt, F. Theiss, A.O. El-Warrak, K. Zlinszky, R. Bettschart-Wolfisberger, M. Bohner, S. Matter, J.A. Auer, B. von Rechenberg, Biomaterials **25**, 1439 (2004). doi:10.1016/j.biomaterials.2003.08.073
- B.R. Constantz, B.M. Barr, I.C. Ison, M.T. Fulmer, J. Baker, L. McKinney, S.B. Goodman, S. Gunasekaran, D.C. Delaney, J. Ross, R.D. Poser, J. Biomed. Mater. Res. **43**, 451 (1998). doi:10.1002/(SICI)1097-4636(199824)43:4<451::AID-JBM13>3.0.CO;2-Q
- M. Francis, N. Webb, Calcif. Tissue Int. **6**, 335 (1970). doi:10.1007/BF02196214
- G.J. Levinskas, W.F. Neuman, J. Phys. Chem. **59**, 164 (1955). doi:10.1021/j150524a017
- B.S. Strates, W.F. Neuman, B.J. Levinskas, J. Phys. Chem. **61**, 279 (1957). doi:10.1021/j150549a005